J. Min. Metall. Sect. B-Metall. 60 (2) (2024) 283 - 293

Journal of Mining and Metallurgy, Section B: Metallurgy

EXPERIMENTAL INVESTIGATION ON WAAM-BASED FUNCTIONAL HARD-FACING BIMETALLIC PART

D.E. Akpınar [a], S. Dilibal [b, c, *], U. Gürol [d]

[a] Department of Mechanical Engineering, Istanbul Gedik University, Türkiye
[b] Department of Mechatronics Engineering, Istanbul Gedik University, Türkiye
[c] Robot Tech. Research & Application Center (RTRAC), Istanbul Gedik University, Türkiye
[d] Department of Metallurgical and Materials Engineering, Istanbul Gedik University, Türkiye

(Received 05 May 2024; Accepted 02 September 2024)

Abstract

In the traditional production of functional bimetallic parts with hard surfaces, the materials for the hard surfaces are usually applied to a base metal, a process that is often complex, costly, and time-consuming. In this paper, the Wire Arc Additive Manufacturing (WAAM) process is proposed as an alternative approach for the production of functional bimetallic parts with hardfacing wire to increase wear resistance. In this study, the hard-facing bimetallic part was fabricated by depositing Hardcor 600 G hardfacing wire onto the deposited 316L Si austenitic stainless steel. After the initial visual inspection and digital X-ray tests, the hardness distribution and macro- and microstructural examinations were carried out. In the subsequent analyses, tensile and Charpy V-notch tests were carried out on the samples taken from the manufactured bimetallic part. The mechanical properties of the functional hard-facing bimetallic parts showed different properties of the bimetallic part, with the Hardcor 600 G side exhibiting higher strength compared to the SS 316L Si side. In addition, the Charpy-V notch test showed a notable difference in impact resistance, with the SS 316L Si side having the highest strength, the Hardcor 600 G side having the lowest strength, and the interface being in between. The results show that the WAAM process is a viable alternative to produce functional bimetallic components with hard surfaces, especially for applications requiring increased wear resistance.

Keywords: *WAAM-based manufacturing; Hardfacing welding wire; Bimetallic Wear-resistant Component; Bimetallic Interface*

1. Introduction

Additive manufacturing (AM) revolutionizes traditional manufacturing processes by enabling the structural construction of industrial components through a layer-by-layer approach [1-3]. As a subset of this broad field, Wire Arc Additive Manufacturing (WAAM) specifically applies AM principles using arc welding technology, merging the flexibility of AM with the efficiency of welding. In this process, wide variety of components are precisely built from CAD models by depositing welding wires in successive layers employing a predefined tool path [4-5].

In this advanced robot-assisted additive manufacturing technique, industrial robots are used as essential instruments with their precise control and maneuver capabilities. They also enable the manufacturing of many different complex geometries, which are beyond the reach of the traditional manufacturing counterparts [6]. Furthermore, the integration of industrial robots in WAAM process not only provides a flexible production process but also decreases the final production cost. Moreover, their integration in the additive manufacturing process increases significantly the design and manufacturing capabilities for conducting innovative AM-based studies [7-9].

In robotic WAAM-based structures, the macroscopic and microscopic characteristics of the deposited products are significantly affected by various welding-based parameters [10]. These parameters include the deposition rate, the welding current mode, type of shielding gas used, the welding wire feed rate, and the applied heat input etc. Critical operational parameters in WAAM include the cooling intervals, interlayer temperature, and solidification rate. Additionally, adjustments to the deposition current, inter-pass temperature, and torch travel speed are vital for achieving desired material properties and dimensional accuracy [11]. Compared with the other

Corresponding author: savas.dilibal@gedik.edu.tr

https://doi.org/10.2298/JMMB240505020A

fusion-based additive manufacturing techniques, WAAM specifically offers the highest deposition rate enabling large-volume production up to 10 kg/h for steel manufacturing process [12].

There are many techniques for manufacturing bi-metallic components such as roll bonding, laser cladding, brazing, diffusion bonding, friction stir welding, TIG welding, electroplating, powder metallurgy, cold spray, and bimetallic casting. Additionally, explosive welding has been widely explored due to its ability to create strong metallurgical bonds between dissimilar metals. In the literature, the microstructural and mechanical properties of explosively welded Al/Cu [13], Al/Stainless steel [14], bronze-carbon steel [15], steel-bronze [16] have been investigated, revealing how these properties are influenced by explosive welding and subsequent heat treatments. However, while explosive welding is effective in producing high-strength bonds, it presents challenges such as the potential for high residual stresses, limited geometric complexity, and safety concerns associated with the explosive materials used.

With the growth of the requirement for customized functional bi-metallic parts in industry, the additive manufacturing of bimetallic components is becoming crucial, especially for producing a variety of functionally graded components. This approach also facilitates the combination of dissimilar metals, which optimizes material properties to enhance functionality and performance in critical applications. The capability to produce bimetallic parts with WAAM opens opportunities for creating structures that are lightweight, high-strength, and corrosion-resistant components. In the literature, Tianying et al. [17] successfully created a bimetallic rocket motor shell with a complex microstructure using the WAAM process. Further contributions include Rodrigues et al. [18] developed a functional copper-steel part, employing advanced twin-wire and GMAW (gas metal arc welding)-based AM process. Recent studies, including those by Ahsan et al. [19], have focused on investigating the microstructural and mechanical properties of ferritic-austenitic bimetallic structures made using WAAM, particularly examining the interface with optical and SEM analyses along with tensile tests. Additionally, Hu et al. [20] developed a WAAM-based bimetallic hierarchical structure using hot-working tool steel RMD535 and martensitic stainless steel RMD650 and explored the enhanced mechanical properties with hard and soft materials. Further exploration by Uralde et al. [21] and Chen et al. [11] into deposition strategies and material interactions revealed that overlapped deposition techniques enhance elongation and reduce stress, while interfaces in laminated structures exhibit a fine-grained microstructure that significantly affects mechanical properties.

Additional studies explored innovative functionally graded bimetallic structures in the literature. Chen et al. [22] utilized a double-feedstock-based arc additive manufacturing process to produce a functionally graded component using TC4 and ER-316L wires as feedstocks. They investigated the evolution of microstructure and micro-hardness based on varying elemental compositions. Montwani et al. [23] deposited a WAAM-based bimetallic thin wall comprising SS316LSi stainless steel and Ni-based IN625 alloy to determine its mechanical properties and microstructure. In the recent study, Dilibal and his coworkers conducted research on bimetallic structures by combining ferritic and austenitic steels to investigate their mechanical properties [24]. They also investigated the bi-metal interface characteristics of the manufactured bimetallic component experimentally. Despite the increased mechanical strength, the bimetal interface exhibited a rapid decrease in fracture toughness in a brittle manner. This phenomenon was attributed to the martensitic phase and carbide precipitations which occurred due to the interactions of the ferritic-austenitic materials at the interface.

In this study, the robotic WAAM process was used for producing functional wear-resistant bimetallic part with Hardcor 600 G and ELOX SG 316L Si welding wires. The manufactured bimetallic wear-resistant part was subjected to detailed microstructural characterization and mechanical testing to reveal its mechanical response and associated hardness-based wear-resistant characteristics.

2. Experimental Procedure

In the experimental setup for the WAAM process, the robotic welding-cell was equipped with the following instruments as shown in Figure 1; a 6-axis OTC Daihen FD-B6L industrial robot, a synergistic welding machine (GeKaMac Power MIG GPS WB P500L), an OPTRIS Xi 400 thermal camera, and an OPTRIS CT 3M pyrometer. The employed synergistic welding machine was initially set to low spatter mode for stable arc and spattering condition. Gas Metal Arc Welding (GMAW)-based WAAM process synergistically combined to produce bi-metallic components experimentally. To build a functional hard-facing bi-metallic part, two different welding wires were employed: GeKaTec 600 G (MSG 6 GZ-60, according to DIN 8555) and GeKa ELOX SG 316 L Si (ER 316 L Si, according to AWS A5.9). A 316 stainless steel base plate with the dimension of 350 mm x 150 mm x 12 mm was employed as a substrate during the deposition. Detailed chemical compositions of both the employed welding wires and the substrate are provided in Table 1.

Table 1. *The obtained chemical analysis for the feedstock and substrate (wt. %)*

	C	Si	Mo	Cr	Ni
ELOX SG 316L Si	0.02	0.80	1.98	18.5	11.50
GeKaTeC 600G	0.4	3	-	9	0.5
Substrate - SS 316L	0.022	0.003	-	16.70	-

In the WAAM process, two different shielding gases, M12 for Hardcor 600 G and M21 for ELOX SG 316L Si welding wire (acc. to EN ISO 14175), were employed during layer-by-layer deposition. To build a thick functional wear-resistant bimetallic part, a total of 60 layers were deposited in three overlapping passes per layer. Initially, 30 layers were applied onto an SS316 substrate using ER 316L Si welding wire, followed by another 30 layers using hard-facing welding wire on the previously deposited layers. Temperature variations in the substrate during deposition were monitored using a pyrometer (Optris CT 3M) and thermal camera (Optris Xi 400), which captured thermal images every five passes and five seconds prior to each deposition. WAAM process parameters for the functional wear-resistant bimetallic part are given in Table 2. The experimental flowchart that was applied in this study for the WAAM-based deposition of hard-facing bimetallic part is shown in Figure 2.

Table 2. *Applied WAAM parameters for the functional wear-resistant bimetallic part*

	Unit	ELOX SG 316L Si	Hardcor 600 G
Applied current	Amp	130-160	150-180
Applied voltage	V	17-19	18-21
Applied torch angle	degree	90	90
Welding speed	cm/min	35-45	35-45
Shielding gas flow rate	l/min	15	15

Figure 3 illustrates the toolpath planning for the WAAM-based deposition process. It demonstrates that the deposition was performed using a parallel deposition method. In this strategy, each layer was welded using three overlapping passes executed in parallel. To prevent macro and microstructural defects resulting from variable heat dissipation at the beginning and end of each layer, the deposition direction was alternated with each layer during the deposition process.

To observe the heat accumulation during the deposition process, the process was monitored using an optical pyrometer and thermal camera. The recorded heat accumulation during the 60-layer deposition process is shown in Figure 4. The continuous deposition characteristic of the WAAM process leads to an accumulation of heat, which in turn decelerates the cooling rate, particularly in the

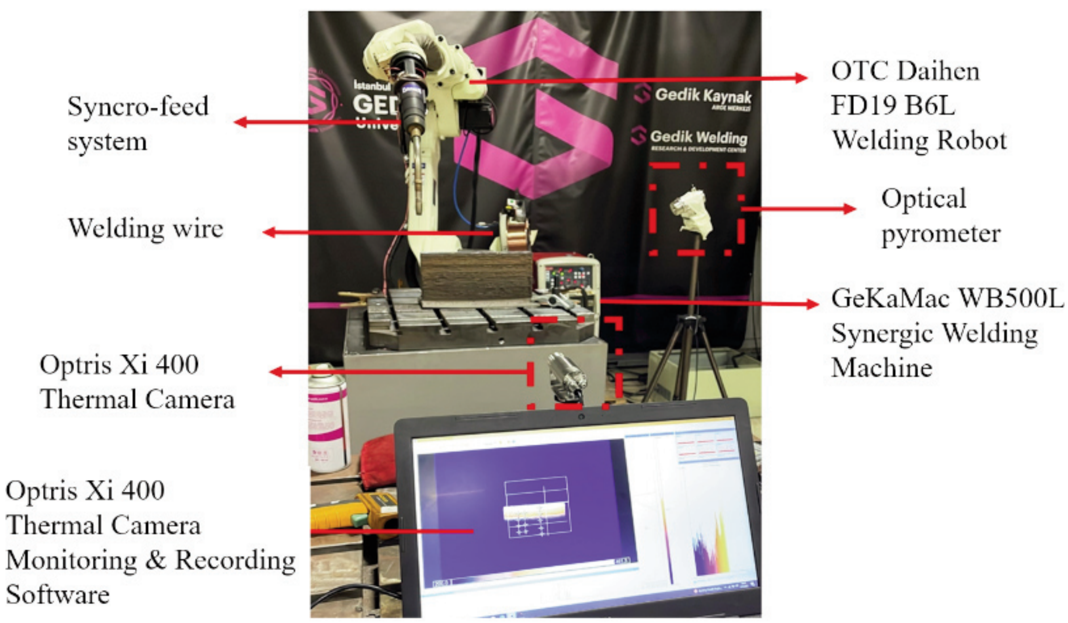

Figure 1. *Experimental setup for the robotic WAAM-based deposition process*

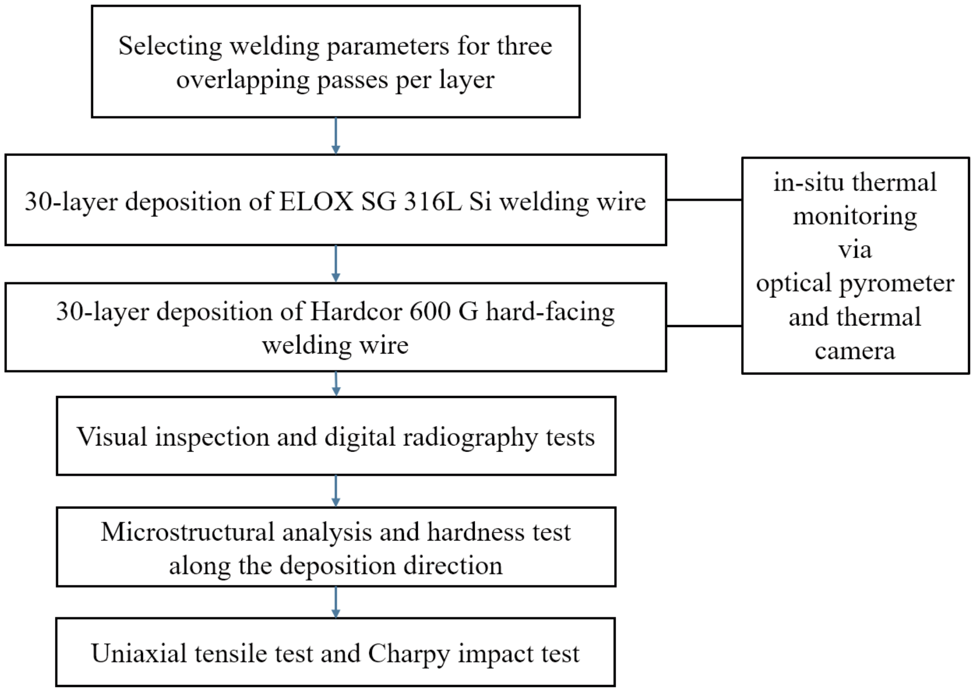

Figure 2. *Experimental flowchart for the WAAM-based deposition of bimetallic part*

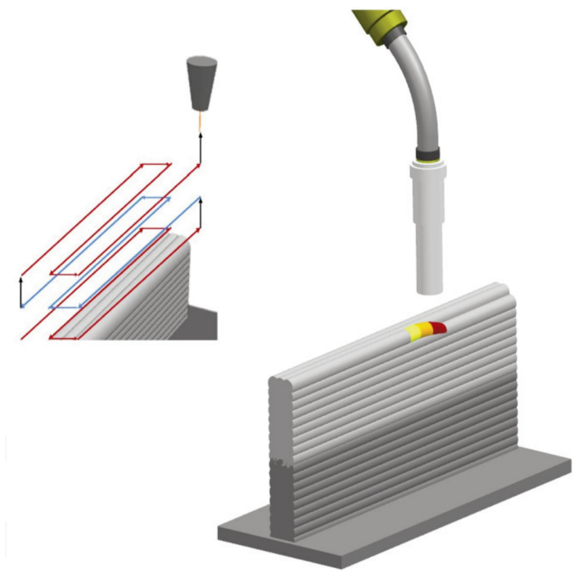

Figure 3. *Toolpath planning for the WAAM-based deposition process of bimetallic part*

upper layers of the structure. To prevent high heat accumulation during the deposition process, the deposition direction was alternated after each layer to prevent the accumulation of material at the start and stop points. Additionally, a cooling interval of 180 seconds between layers was implemented as a dwell time, allowing the deposited part to cool.

Digital radiography tests aligned with EN ISO 17636-2 were conducted to identify any potential interlayer defects such as micro-cracks, porosity in the manufactured wear-resistant functional bimetallic component. Microstructural alterations, dependent on location, were examined using an optical microscope (OM). The mechanical properties, including hardness distribution, tensile strength, and Charpy V-notch-based impact toughness, were evaluated at three different sections, including the interface, ELOX SG 316L Si and Hardcor 600 G regions as shown in Figure 5. The samples which were extracted from the deposited bimetallic part via electrical discharge

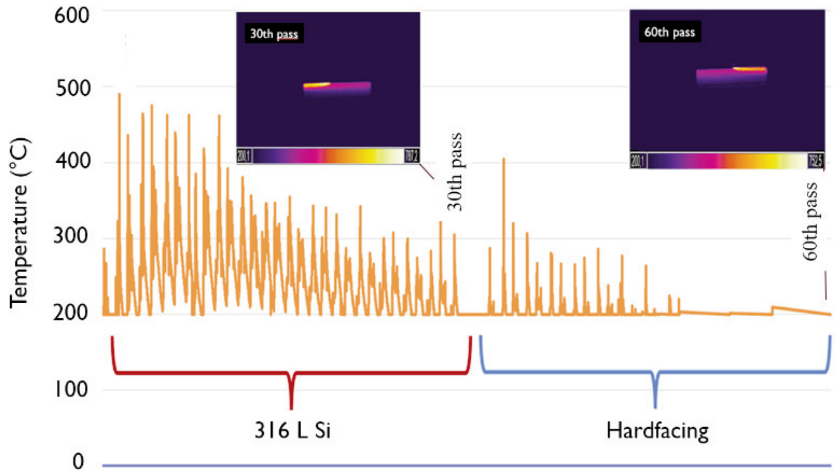

Figure 4. *The recorded heat accumulation during the 60-layer deposition process*

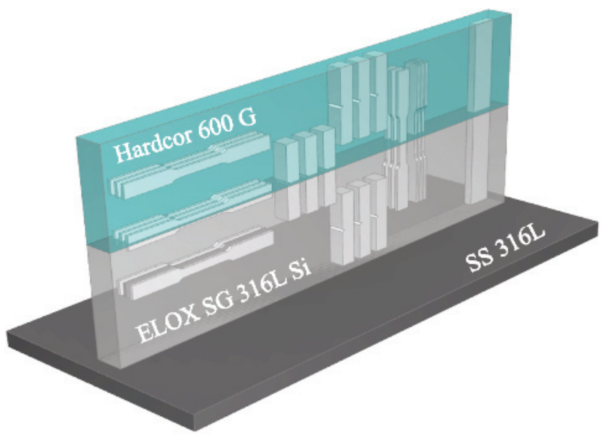

Figure 5. *Locations of the extracted specimens from the deposited bimetallic part*

machining (EDM) examined for micro-hardness along a polished cross-section to detect local hardness variations potentially caused by the overlapping deposition process.

Micro-hardness related evaluations were executed on as-polished cross-sections along the central vertical axis, adhering to EN ISO 9015, employing a fully automated hardness device utilizing the Vickers (HV) method with a force parameter of 1 kg. The preparation of cross-sectional samples, including grinding, polishing, and etching, was conducted according to the EN ISO 17639. Two different etchants were utilized for the Hardcor 600 G and ELOX SG 316L Si layers within the bimetallic part to determine their distinct microstructures. Uniaxial tensile tests were performed at room temperature utilizing sub-size flat-type tensile specimens in accordance with the ASTM E8 and EN ISO 9016 standards. Additionally, the fractured surface of Charpy specimens was examined using a stereo microscope (SM).

3. Experimental results

Visual inspection along with the X-ray analysis validated the successful melting of both deposited welding wires through a stable arc during the robotic WAAM process, with no internal or surface defects surpassing EN ISO 5817-B tolerances as shown in Figure 6. To determine the dimensions of the hard-facing bimetallic part, measurements were taken from five points, resulting in an average length of 330 mm, height of 150 mm, and thickness of 18 mm.

The macroscopic cross-section of the thick functional hard-facing bimetallic part, depicted at the middle of Figure 7, consists of layers of stainless steel at the bottom and Hardcor 600G wire at the top. Upon examining microstructural changes in three different regions, at the bi-metallic interface, a partially mixed zone without any micro-cracks is noted regionally (Figure 7a, b). The presence of segregation zones is clearly seen at the interface due to elemental diffusion. Moving upwards towards the Hardcor

600G region from the interface, an increase in the quantity and thickness of carbides along grain boundaries (indicated by black regions) is observed. Additionally, as the dilution rate decreases towards the Hardcor 600G region, the structure transforms into one containing carbide along grain boundaries throughout the martensitic matrix (Figure 7c). In the SS 316L Si region, it is observed that various types of delta ferrite phases (predominantly skeletal ferrite type) form parallel to heat accumulation due to high Cr-Ni content (Figure 7d).

Hardness measurements were obtained at a total of 120 locations, with 80 points sampled from the austenitic stainless steel (ELOX SG 316L Si) region and 40 points from the Hardcor 600 G region, with intervals of 0.25 mm. The measured hardness values remain totally consistent starting from the 316L Si stainless steel region to the interface but gradually increase at the interface, surpassing 700 HV as shown in Figure 8. This gradual increase can be attributed to the higher carbon content in the hard-facing wire, which facilitates the formation of martensitic structure

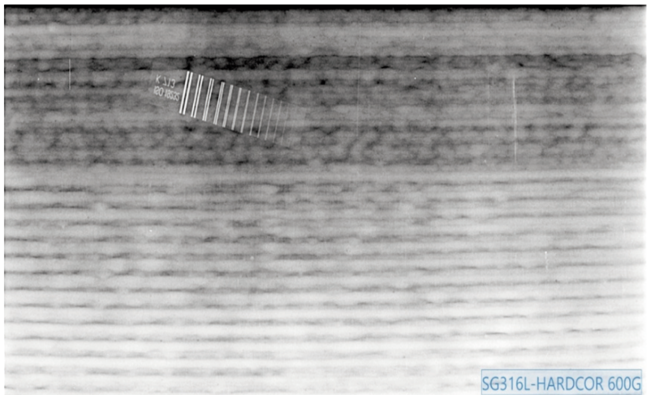

Figure 6. *The digital radiography test result*

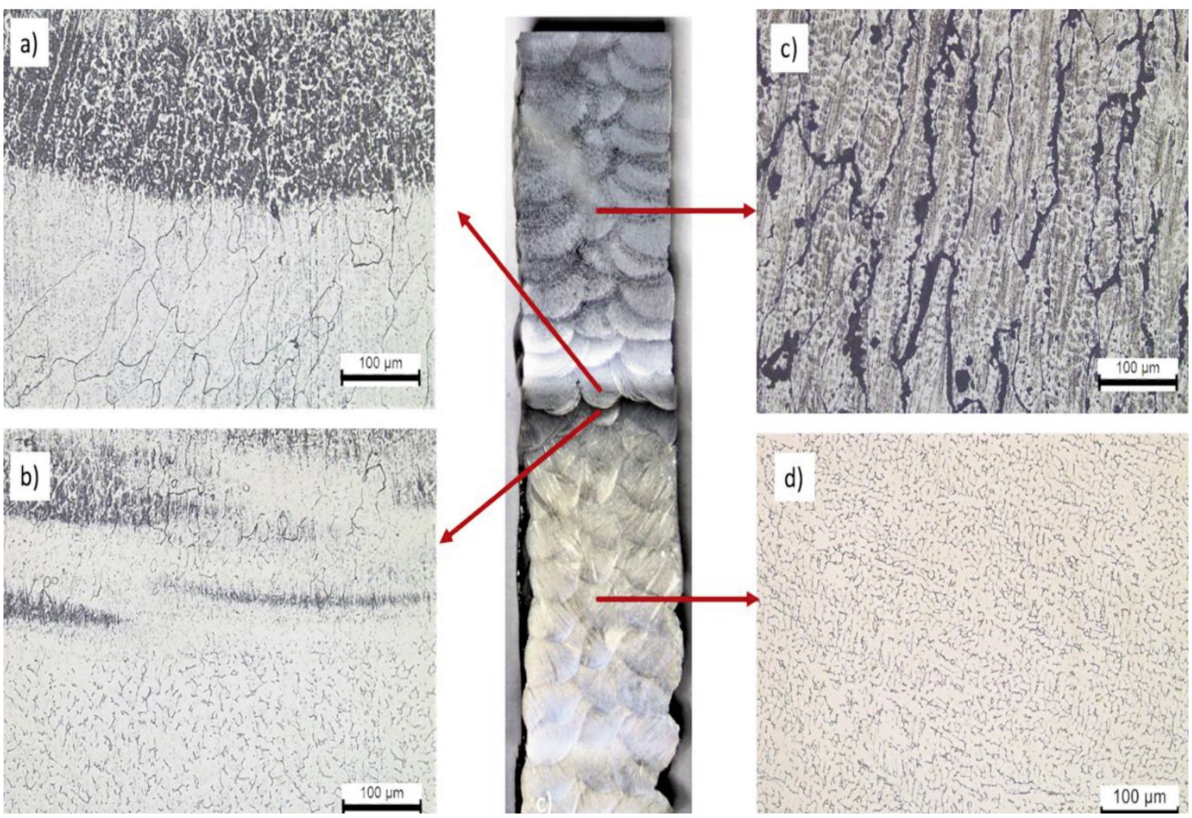

Figure 7. *The macro and microstructure of as-built functional hard-facing bimetallic part a, b) Interface, c) Hard-facing (600 G) side d) 316L stainless steel side*

and chrome carbides in this region. The changes in hardness on the hard-facing side can be attributed to the variation in temperature during the deposition, affecting the cooling rate, solidification and microstructural formation.

The uniaxial tensile test results, derived from the stress-strain curves obtained, are presented in Table 3. The table displays the average stress-strain curves obtained from three test specimens extracted from each region. Based on the findings presented in Table 3, several key observations can be drawn regarding the uniaxial tensile test results of the specimens extracted from different regions. The samples from the hard-facing side demonstrated the highest yield and tensile strengths, reaching 814 MPa and 1337 MPa, respectively. However, this was accompanied by the lowest elongation at 1.5%, attributed to the presence of metal carbides within the martensitic matrix. In contrast to the lowest elongation at the hard-facing side, specimens from the 316L Si stainless steel side exhibited the highest elongation at 33.8%, indicating higher ductility in this stainless-steel region. The samples extracted from the bimetallic interface region displayed the lowest yield and tensile strengths with the values of 326 MPa and 463 MPa, respectively.

The received uniaxial tensile test results emphasize the effect of microstructural composition on the mechanical response of the deposited bimetallic part. The occurrence of metal carbides in the hard-facing side of the bimetallic part contributed to obtain an enhanced strength but reduced ductility, whereas the 316L Si austenitic stainless-steel side demonstrated highest ductility despite lower strength values. The bimetal interface, characterized by a combination of both hard-facing and 316L Si austenitic stainless-steel materials, exhibited intermediate mechanical properties.

Figure 9a. shows the measured Charpy impact test results of the extracted samples from austenitic stainless steel, bimetallic interface and hard-facing sides of the deposited part. The samples received from the 316L Si austenitic stainless-steel side displayed the highest impact energy. In contrast, the Hardcor 600G side exhibited the lowest impact energy, which contrasts with the results observed from the 316L Si austenitic stainless-steel side. The highest Charpy-V notch test results were achieved at 152 ± 14 J on the SS 316L Si side, while registering significantly lower values of 5 ± 1 J on the Hardcor 600 G side. As anticipated, the interface displayed an intermediate value of 96 ± 32 J. Moreover, the interface specimen demonstrated a notable reduction of approximately 55% (54 ± 9 J) in fracture toughness values compared to the SS 316L side.

The fracture direction of the interface sample was examined after the Charpy impact test. The samples were milled 2 mm perpendicular to the notch direction and then encased in Bakelite. The sample encased in Bakelite was sanded with 120, 220, 320, 600 and 800

Table 3. *The tensile test results for the deposited wear-resistant bimetallic part*

	Yield strength (MPa)	Tensile strength (MPa)	Elongation (%)
SS 316 L Si	338	580	33.8
Bimetallic interface	326	463	3.5
Hardcor 600 G	814	1337	1.5

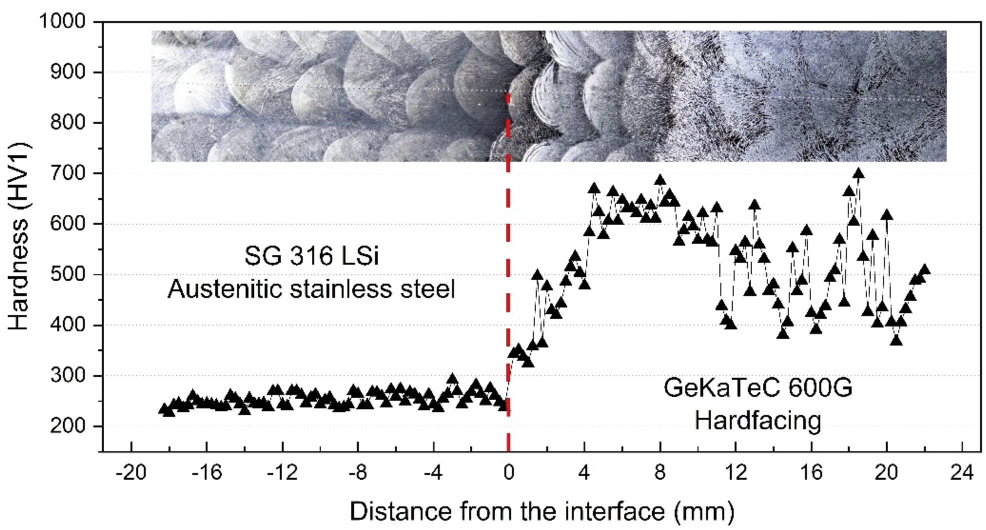

Figure 8. *Hardness (HV1) variation along the deposition direction*

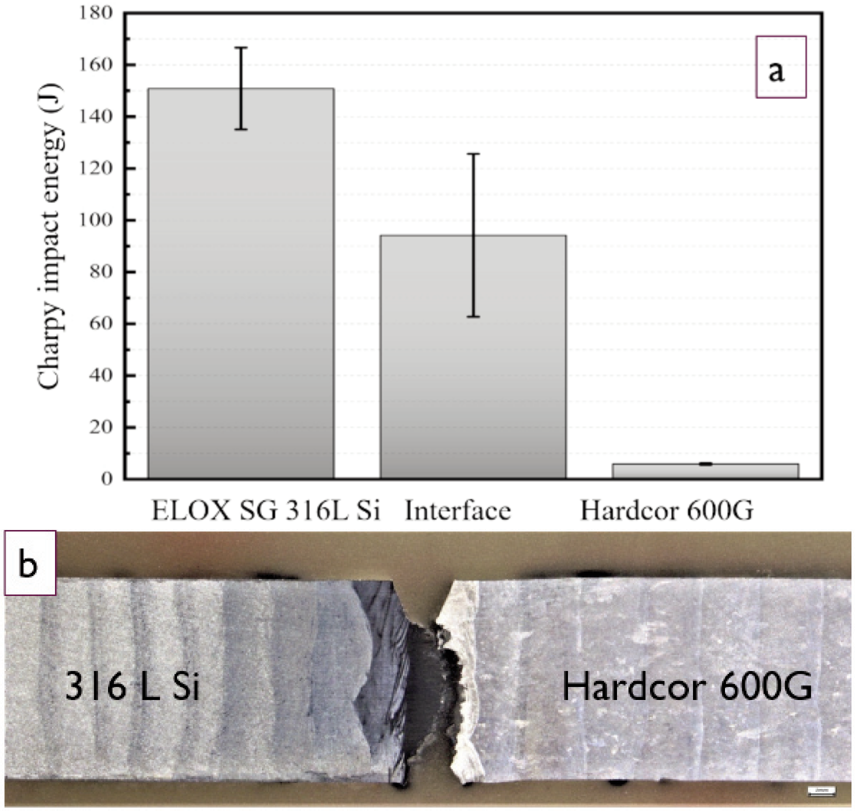

Figure 9. *a) Charpy impact test result of the wear-resistant bimetallic part, b) Charpy specimen' cross-sectional view with the interface displaying the crack propagation*

grit, respectively using the Metkon Forcipol 2V sanding device and etched with FeCl3. After the metallographic preparation processes, macro images were taken from the sample.

The Charpy impact test results presented in Figure 6a highlight notable differences in impact energy among samples extracted from austenitic stainless steel, bimetallic interface and hard-facing regions of the deposited part. Specifically, specimens from the 316L Si austenitic stainless-steel side exhibited the highest impact energy, while those from the Hardcor 600G side displayed the lowest. This discrepancy contrasts with the results observed from the austenitic stainless-steel side, indicating distinct mechanical behavior between the materials. Upon examination of the fracture direction of the interface sample post-Charpy impact test, it was observed that the crack propagated along the bimetallic interface, as depicted in Figure 9b. This observation aligns with expectations, as the Charpy specimen extracted from the bimetallic interface was found to have fractured from the 316L Si stainless steel side. The crack propagation along the bimetallic interface highlights the critical role of interface integrity in determining the overall mechanical performance of bimetallic components. It is noteworthy that the microstructural composition of the bimetallic part influences the determination of its impact energy and toughness properties. The reduced impact energy in the hard-facing side of the bimetallic part is linked to its microstructure and hardness characteristics. The measured high hardness values indicate the potential to decrease both ductility and toughness, thereby limiting the material's energy absorption capacity to under impact conditions.

4. Conclusions

In this study, a functional wear-resistant bimetallic part was manufactured using ELOX SG 316L Si and Hardcor 600 G welding wires through robotic WAAM technology. The microstructure and mechanical properties of the wear-resistant bimetallic structure were characterized using radiographic analysis, Vickers hardness, optical microscopy, tensile, and Charpy V-notch tests. The main conclusions are summarized below.

a) A functional wear-resistant bimetallic WAAM part has been successfully fabricated using a GMAW-based WAAM process, exhibiting no weld defects, cracks, or porosity. Detailed examination of the interlayer interfaces showed that they are well-bonded without any defects, enabling the built of wear-resistant bimetallic part.

b) The hardness analysis validated the effectiveness of the WAAM process in producing wear-resistant bimetallic components, with desirable hardness values of 711 HV on the Hardcor 600 G side and 204 HV on the 316L Si side. The consistent hardness values observed across the bimetallic part, coupled with the gradual increase towards the interface and exceeding 700 HV, are attributed to the higher carbon content in the hard-facing wire, which promotes the formation of a martensitic structure.

c) The tensile test results revealed distinct mechanical behavior among specimens extracted from different regions of the bimetallic part. The hard-facing side exhibits superior strength with reduced ductility compared to the 316L Si stainless steel side. Conversely, the interface region displays intermediate mechanical properties.

d) The Charpy-V notch test results uncovered a substantial variation in impact energy distribution across different regions of the bimetallic part, with the SS 316L Si side exhibiting the highest impact resistance at approximately 152 ± 14 J, while the Hardcor 600 G side showed significantly lower values of 5 ± 1 J. Additionally, the interface exhibited an intermediate impact energy level of 96 ± 32 J

e) This study demonstrated that WAAM is a potential alternative to conventional cladding methods, offering enhanced wear resistance and material customization in manufacturing processes. Future investigations will focus on designing and manufacturing a functional bimetallic industrial component which can be used for wear-resistant purposes.

Acknowledgements

This study was funded by the Turkish Scientific & Technological Research Council (TUBITAK) with the project no. 5220023 under the support program of industry-university cooperation.

Competing interest

There is no conflict of interest among the authors.

Author contributions

Conceptualization D.E.A., S.D. and U.G.; experimental work D.E.A.; writing-review and editing, S.D. and U.G. supervision, and validation S.D. and U.G.

Data availability

Data sharing is not applicable for this study.

References

[1] L. Huang, X. Chen, S. Konovalov, C. Su, P. Fan, Y. Wang, P. Xiaoming, I. Panchenko, A review of challenges for wire and arc additive manufacturing (WAAM), Transactions of the Indian Institute of Metals, 76 (2023) 1123–1139. https://doi.org/10.1007/s12666-022-02823-y

[2] H. Pant, A. Arora, G.S. Gopakumar, U. Chadha, A. Saeidi, A.E. Patterson, Applications of wire arc additive manufacturing (WAAM) for aerospace component manufacturing, The International Journal of Advanced Manufacturing Technology, 127 (2023) 4995–5011. https://doi.org/10.1007/s00170-023-11623-7

[3] G. Peduk, S. Dilibal, O. Harrysson, S. Ozbek, Experimental investigation on the EBM-Based additively manufactured prismatic nickel–titanium SMA components, Russian Journal of Non-Ferrous Metals, 62 (3) (2021) 357–367. http://doi.org/10.3103/S1067821221030020

[4] M. Chaturvedi, E. Scutelnicu, C.C. Rusu, L.R. Mistodie, D. Mihailescu, A.V. Subbiah, Wire arc additive manufacturing: Review on recent findings and challenges in industrial applications and materials characterization, Metals, 11(6) (2021) 939. https://doi.org /10.3390/met11060939

[5] D. Ding, Z. Pan, D. Cuiuri, H. Li, A multi-bead overlapping model for robotic wire and arc additive manufacturing (WAAM), Robotics and Computer-Integrated Manufacturing, 31 (2015) 101-110. https://doi.org/10.1016/j.rcim.2014.08.008

[6] U. Gurol, E. Kocaman, S. Dilibal, M. Kocak, A comparative study on the microstructure, mechanical properties, wear and corrosion behaviors of SS 316 austenitic stainless steels manufactured by casting and WAAM technologies, CIRP Journal of Manufacturing Science and Technology, 47 (2023) 215-227. https://doi.org/10.1016/j.cirpj.2023.10.005

[7] W. Zhai, Y. Guo, C. Canturri, R. Shandro, W. Zhou, Wire arc additive manufacturing of ER70S-6/S355 bimetal component, Materials Science and Engineering: A, 900 (2024) 146498. https://doi.org/10.1016/j.msea.2024.146498

[8] R. Sasikumar, A.R. Kannan, S.M. Kumar, R. Pramod, N.P. Kumar, N.S. Shanmugam, Y. Palguna, S. Sivankalai, Wire arc additive manufacturing of functionally graded material with SS 316L and IN625: Microstructural and mechanical perspectives, CIRP Journal of Manufacturing Science and Technology, 38 (2022) 230–242. https://doi.org/10.1016/j.cirpj.2022. 05.005 24

[9] U. Gurol, S. Dilibal, B. Turgut, H. Baykal, H. Kumek, M. Kocak, Manufacturing and characterization of WAAM-based bimetallic cutting tool, International Journal of 3D Printing Technologies and Digital Industry, 6(3) (2022) 548–555. https://doi:10.46519/ij3dptdi.1210836

[10] U. Gurol, M. Tumer, S. Dilibal, Experimental investigation of wire arc additively manufactured Inconel 625 superalloy, Transactions of the Indian

Institute of Metals, 76(5) (2023) 1371– 1379. https://doi.org/10.1007/s12666-022-02797-x 36

[11] Y. Chen, X. Zuo, W. Zhang, Z. Hao, Y. Li, Z. Luo, S. Ao, Enhanced strength-ductility synergy of bimetallic laminated steel structure of 304 stainless steel and low-carbon steel fabricated by wire and arc additive manufacturing, Materials Science and Engineering: A, 856 (2022) 143984. https://doi.org/10.1016/j.msea.2022.143984 28

[12] V.T. Le, M.C. Bui, T.D. Nguyen, V.A. Nguyen, V.C. Nguyen, On the connection of the heat input to the forming quality in wire-and-arc additive manufacturing of stainless steels, Vacuum, 209 (2023) 111807. https://doi.org/10.1016/j.vacuum.2023.111807

[13] M.R. Jandaghi, A. Saboori, G. Khalaj, M. Khanzadeh Ghareh Shiran, Microstructural evolutions and its impact on the corrosion behavior of explosively welded Al/Cu bimetal, Metals, 10(5) 634 (2020). https://doi.org/10.3390/met10050634

[14] S.F. Shargh, A. Saadat, A. Najafi, M.R.K. Gharehshiran, G. Khalaj, Investigating the effect of post weld heat treatment on corrosion properties of explosive bonded interface of AA5083/AA1050/SS 321 tubes, Materials Research Express, 7 (2020) 036529. http://doi.org/10.1088/2053-1591/ab8095

[15] K.G.M. Reza, A. Khoshakhlagh, G. Khalaj, H. Bakhtiari, A.R. Banihashemi, Effect of postweld heat treatment on interface microstructure and metallurgical properties of explosively welded bronze-carbon steel, Journal of Central South University, 25 (2018) 1849–1861. https://doi.org/10.1007/s11771-018-3874-9

[16] G. Khalaj, M. Moradi, E. Asadian, Exploring the impact of rolling temperature on interface microstructure and mechanical properties of steel–bronze explosive welded bilayer composite sheets, Welding in the World, 67 (2023) 1411-1425. https://doi.org/10.1007/s40194-023-01495-6

[17] H. Tianying, Y. Shengfu, R. Yu, B. Zheng, Oscillating wire arc additive manufacture of rocket motor bimetallic conical shell, International Journal of Advanced Manufacturing Technology, 119 (2022) 6601–6612. https://doi. org/10.1007/s00170- 021-08477-2

[18] T.A. Rodrigues, N. Bairrao, F.W.C. Farias, A. Shamsolhodaei, J. Shen, N. Zhou, E. Maawad, N. Schell, T.G. Santos, J.P. Oliveira, Steel-copper functionally graded material produced by twin-wire and arc additive manufacturing (T-WAAM), Materials & Design, 213 (2022) 110270. https://doi.org/ 10. 1016/j. matdes.2021.110270

[19] R.U. Ahsan, A.N.M. Tanvir, T. Ross, A. Elsawy, M. Oh, D.B. Kim, Fabrication of bimetallic additively manufactured structure (BAMS) of low carbon steel and 316L austenitic stainless steel with wire + arc additive manufacturing, Rapid Prototyping Journal, 26(3) (2020) 519–530. https://doi.org/10.1108/RPJ-09-2018-023525

[20] Z. Hu, L. Hua, M. Ni, F. Ji, X. Qin, Microstructure and mechanical properties of directed energy deposition-arc/wire bimetallic hierarchical structures of hot-working tool steel and martensitic stainless steel, Additive Manufacturing, 67 (2023) 103495. https:// doi.org/10.1016/j.addma.2023.103495

[21] V. Uralde, A. Suarez, E. Aldalur, F. Veiga, T. Ballesteros, Wall fabrication by direct energy deposition (DED) combining mild steel (ER70) and stainless steel (SS 316L): Microstructure and mechanical properties, Materials, 15(17) (2021) 5828. https://doi.org/10.3390/ma15175828

[22] X. Chen, J. Han, J. Wang, Y. Cai, G. Zhang, L. Lu, Y. Xin, Y. Tian, A functionally graded material from TC4 to 316L stainless steel fabricated by double-wire + arc additive manufacturing, Materials Letters, 300 (2021) 130141. https://doi.org/ 10.1016/j.matlet.2021. 130141

[23] A. Motwani, A. Kumar, Y. Puri, N.K. Lautre, Mechanical characteristics and microstructural investigation of CMT deposited bimetallic SS316LSi-IN625 thin wall for WAAM, Welding in the World, (2022). https://doi.org/10.1007/s40194-022- 01403-4

[24] U. Gurol, B. Turgut, H. Kumek, S. Dilibal, M. Kocak, Fabrication and characterization of wire arc additively manufactured ferritic-austenitic bimetallic structure, Metals and Materials International, 30 (2023) 1342–1355. https://doi.org/10.1007/s12540-023-01568-7

EKSPERIMENTALNO ISTRAŽIVANJE BIMETALNIH DELOVA SA FUNKCIONALNOM TVRDOM POVRŠINOM PROIZVEDENIH WAAM METODOM

D.E. Akpınar [a], S. Dilibal [b, c, *], U. Gürol [d]

[a] Katedra za mašinsko inženjerstvo, Univerzitet Gedik u Istanbulu, Turska
[b] Katedra za mehatroniku, Univerzitet Gedik u Istanbulu, Turska
[c] Centar za istraživanje i primenu robotskih tehnologija (RTRAC), Univerzitet Gedik u Istanbulu, Turska
[d] Katedra za metalurško i materijalsko inženjerstvo, Univerzitet Gedik u Istanbulu, Turska

Apstrakt

U tradicionalnoj proizvodnji funkcionalnih bimetalnih delova sa tvrdim površinama, materijali za tvrdu površinu obično se nanose na osnovni metal, što je često složen, skup i vremenski zahtevan proces. U ovom radu predložen je proces aditivne proizvodnje žicom (WAAM) kao alternativni pristup za proizvodnju funkcionalnih bimetalnih delova sa tvrdim slojem, kako bi se povećala otpornost na habanje. U ovoj studiji, bimetalni deo sa tvrdom površinom je izrađen taloženjem Hardcor 600 G žice za tvrde slojeve na deponovani 316L Si austenitni nerđajući čelik. Nakon početnog vizuelnog pregleda i digitalnih rendgenskih testova, sprovedena su ispitivanja raspodele tvrdoće, kao i makro- i mikrostrukturalne analize. Nakon toga sprovedeni su zatezni testovi i Charpy V-notch ispitivanja na uzorcima uzetim iz proizvedenog bimetalnog dela. Mehanička svojstva funkcionalnih bimetalnih delova sa tvrdom površinom pokazala su različite karakteristike, pri čemu je strana sa Hardcor 600 G imala veću čvrstoću u poređenju sa stranom SS 316L Si. Pored toga, Charpy-V notch test je pokazao značajnu razliku u udarnoj žilavosti, pri čemu je strana SS 316L Si imala najveću čvrstoću, strana Hardcor 600 G najmanju, dok je vrednost za međusloj bila između. Rezultati pokazuju da je WAAM proces održiva alternativa za proizvodnju funkcionalnih bimetalnih komponenti sa tvrdim površinama, posebno za primene koje zahtevaju povećanu otpornost na habanje.

Ključne reči: *WAAM proizvodnja; Tvrdi sloj za zavarivanje; Bimetalna komponenta otporna na habanje; Bimetalni međusloj*